Supplement of Atmos. Chem. Phys., 16, 9805–9830, 2016
http://www.atmos-chem-phys.net/16/9805/2016/
doi:10.5194/acp-16-9805-2016-supplement

Atmospheric Chemistry and Physics Open Access EGU

Supplement of

Fluorescent biological aerosol particle measurements at a tropical high-altitude site in southern India during the southwest monsoon season

A. E. Valsan et al.

Correspondence to: A. E. Valsan (aswathyerat@gmail.com) and S. S. Gunthe (s.gunthe@iitm.ac.in)

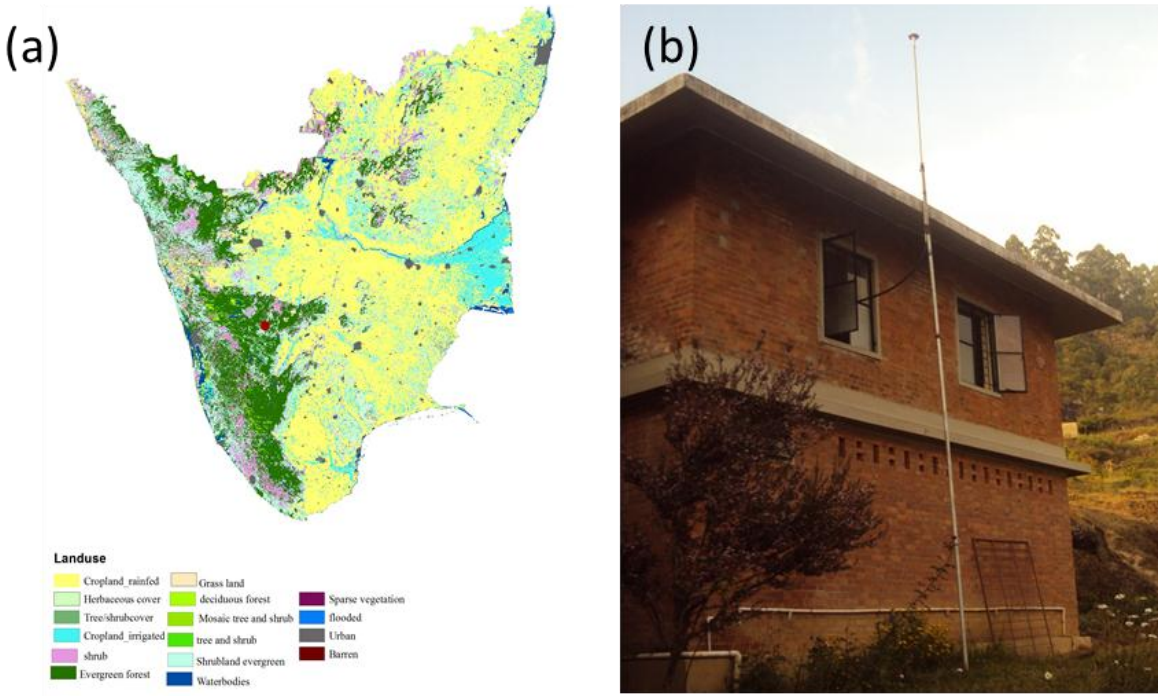

Fig S1: Land use map of the Munnar (a) and UV-APS inlet (b)

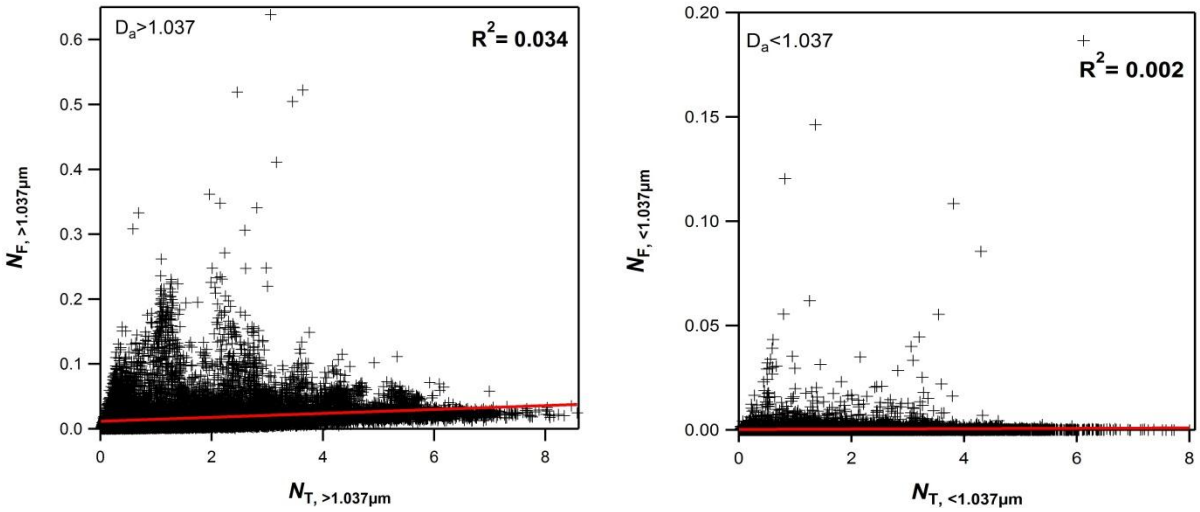

Fig S2: Scatter plots of N_F vs. N_T for particle diameters above **(a)** and below **(b)** 1.0 µm, respectively for the entire campaign. $N_{F,<1.037}$ particle number exhibiting fluorescence in the fine particle mode (< 1.0 µm) and $N_{T,<1.037}$ all particles in size mode. $N_{F,>1.037}$ and $N_{T,>1.037}$, represent coarse mode (> 1.0 µm).

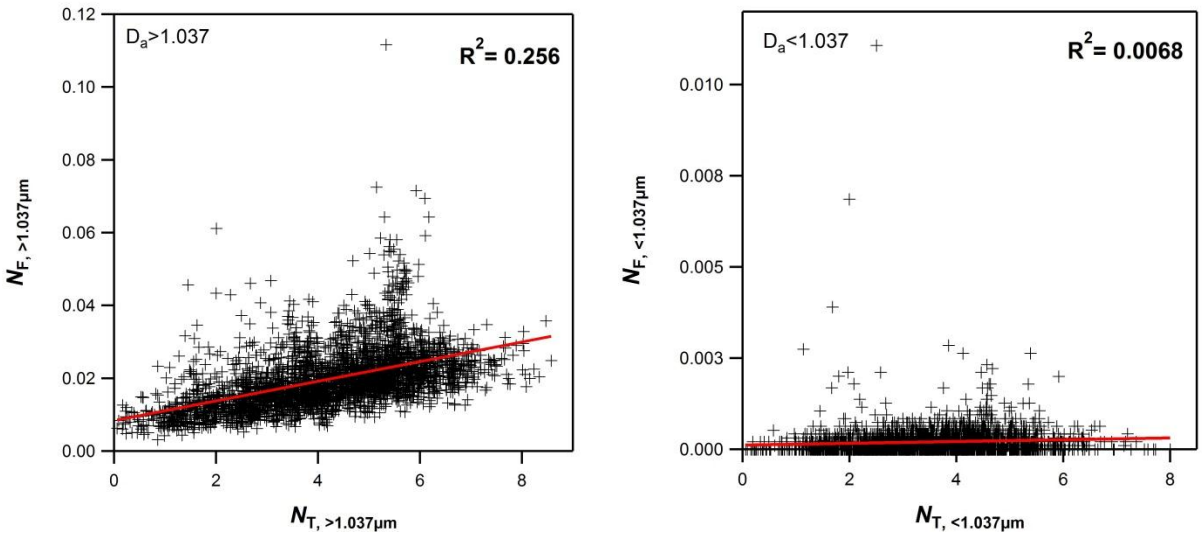

Fig S3: Scatter plots of N_F vs. N_T for particle diameters above **(a)** and below **(b)** 1.0 µm, respectively during dusty period. $N_{F,<1.037}$ particle number exhibiting fluorescence in the fine particle mode (< 1.0 µm) and $N_{T,<1.037}$ all particles in size mode. $N_{F,>1.037}$ and $N_{T,>1.037}$, represent coarse mode (> 1.0 µm).

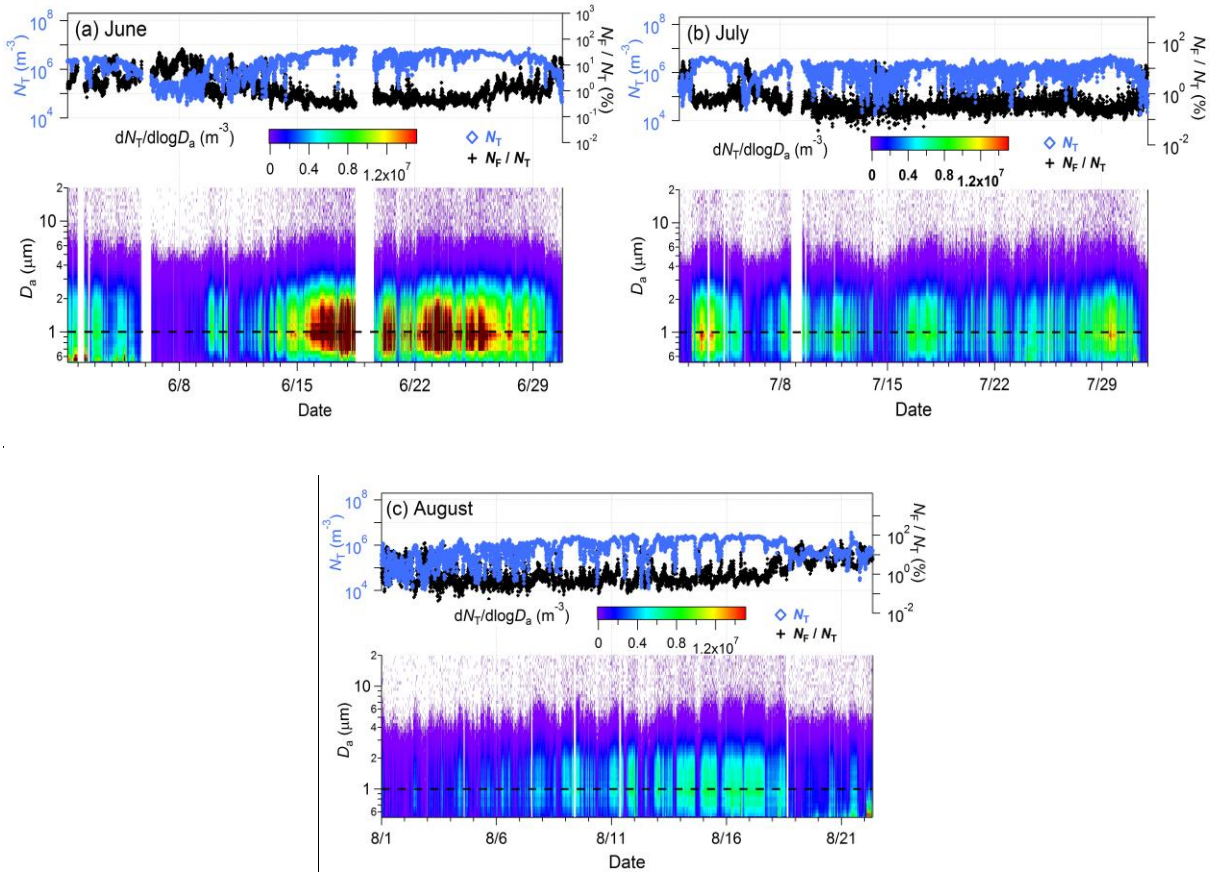

S4: Time series of total particle concentration (blue) and ratio of fluorescent to total particles (black) along with size resolved measurements (lower panel) for each individual months (Jun-Aug)

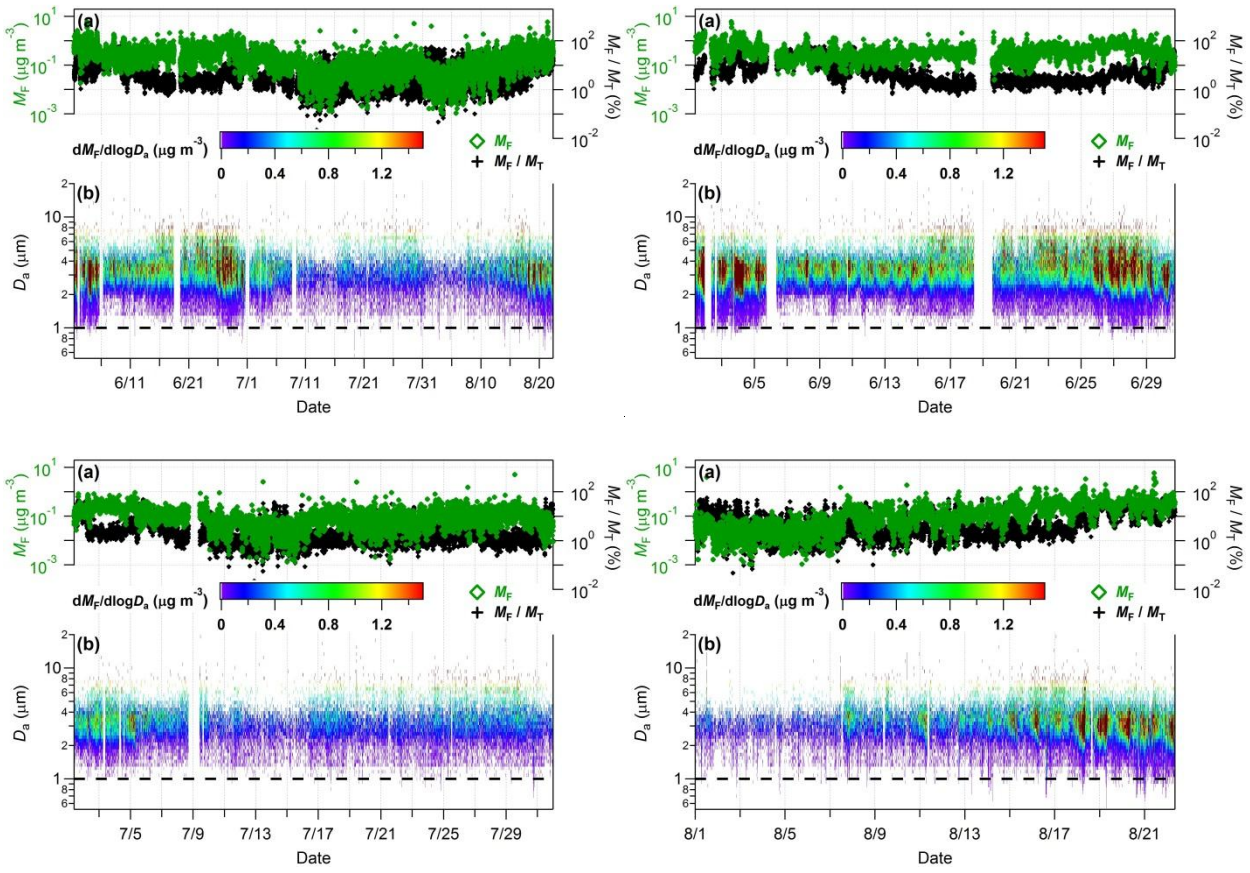

S5: Time series of fluorescent particle mass concentration (green) and ratio of fluorescent to total particles (black) along with size resolved measurements (lower panel) for each individual months (Jun-Aug).

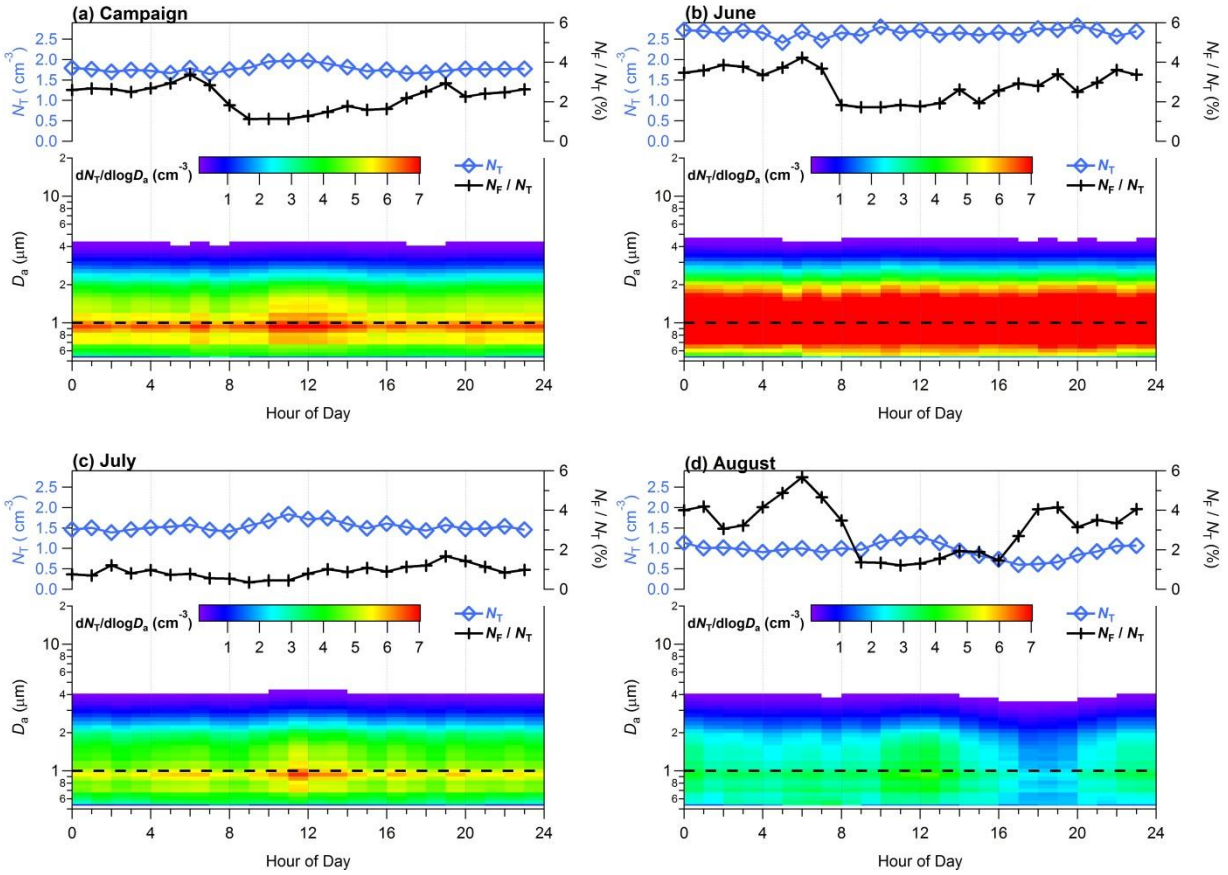

Fig S6: Diurnal cycles of TAP number concentrations (N_T) and size distributions averaged over individual month of measurement and entire campaign (hourly median values plotted against the local time of the day). Upper portion of each panel shows integrated TAP number concentration (~1 – 20 μm; N_F) on the left axis (blue color) and FBAP fraction of TAP number (N_F/N_T) on the right axis (black color). Lower portion of each panel TAP number size distribution (3-D plot) plotted against hour of the day on x-axis, aerodynamic diameter on y-axis and color is scaled for dN_F/dlog D_a indicates the concentration. (a) Averaged over entire campaign, (b) Jun, (c) Jul, and (d) Aug.

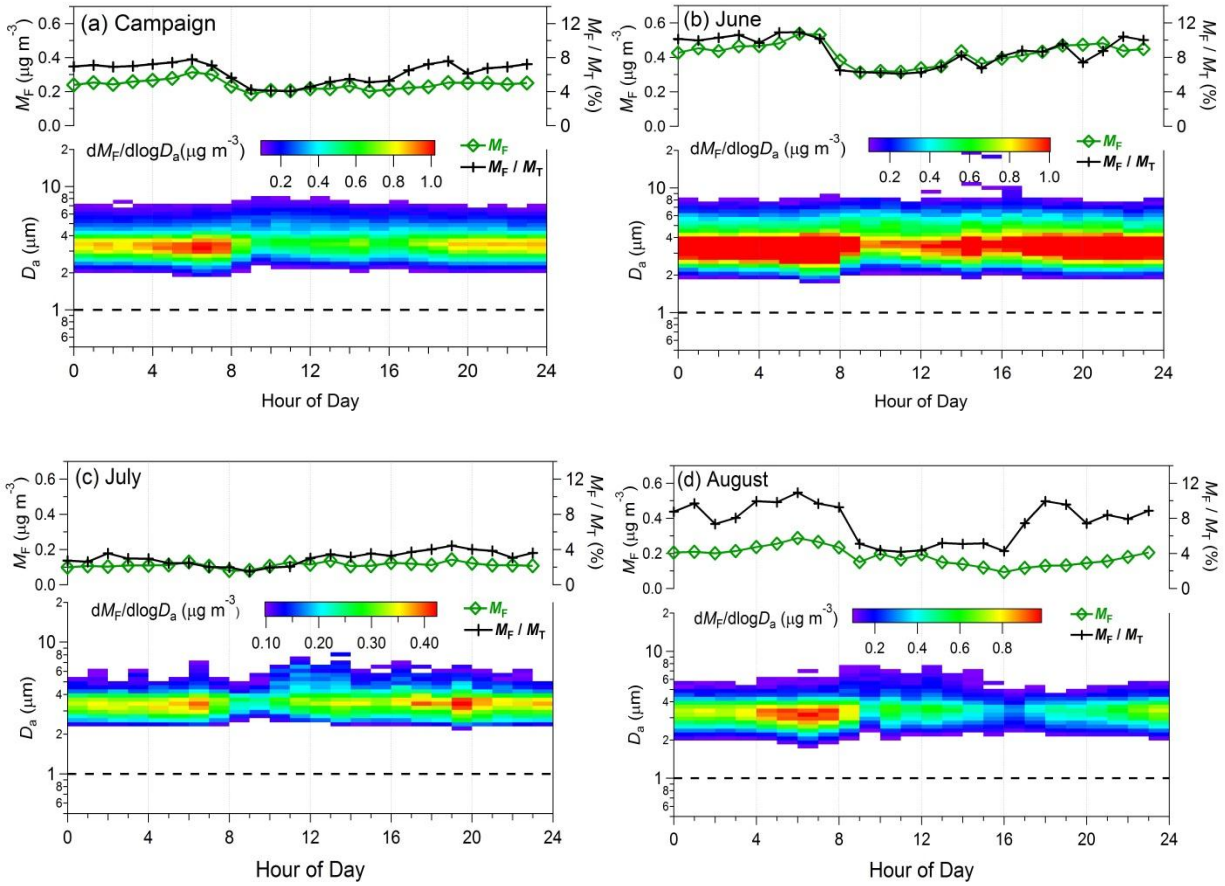

Figure S7: Same as Fig. 4 but representing the FBAP (M_F) mass concentrations.

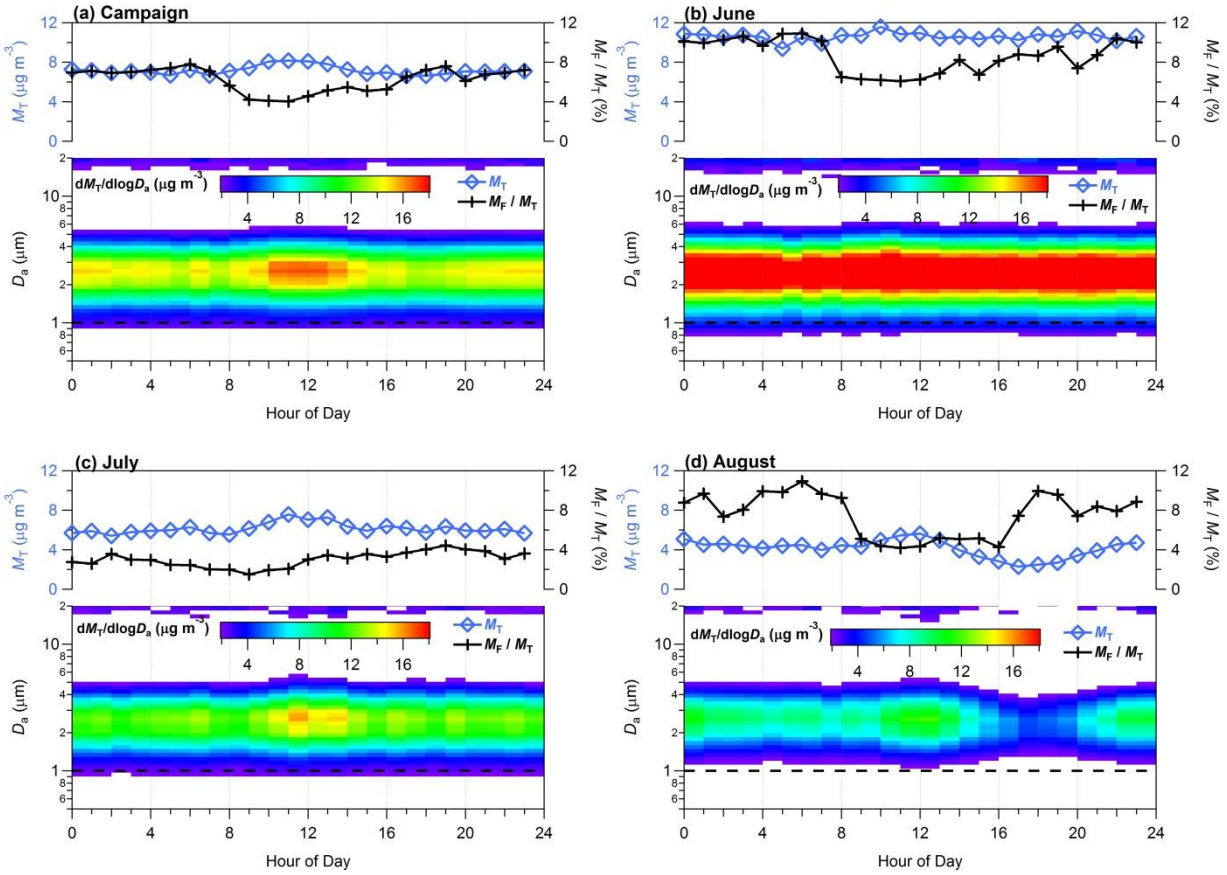

S8. Diurnal cycles of TAP mass concentrations (N_F) and size distributions averaged over individual month of measurement and entire campaign. Upper portion of each panel shows integrated TAP mass concentration (~1 – 20 μm; M_T) on the left axis (blue color) and FBAP fraction of TAP mass (M_F/M_T) on the right axis (black color). Lower portion of each panel FBAP number size distribution (3-D plot) plotted against hour of the day on x-axis, aerodynamic diameter on y-axis and color is scaled for $dM_F/d\log D_a$ indicates the concentration.

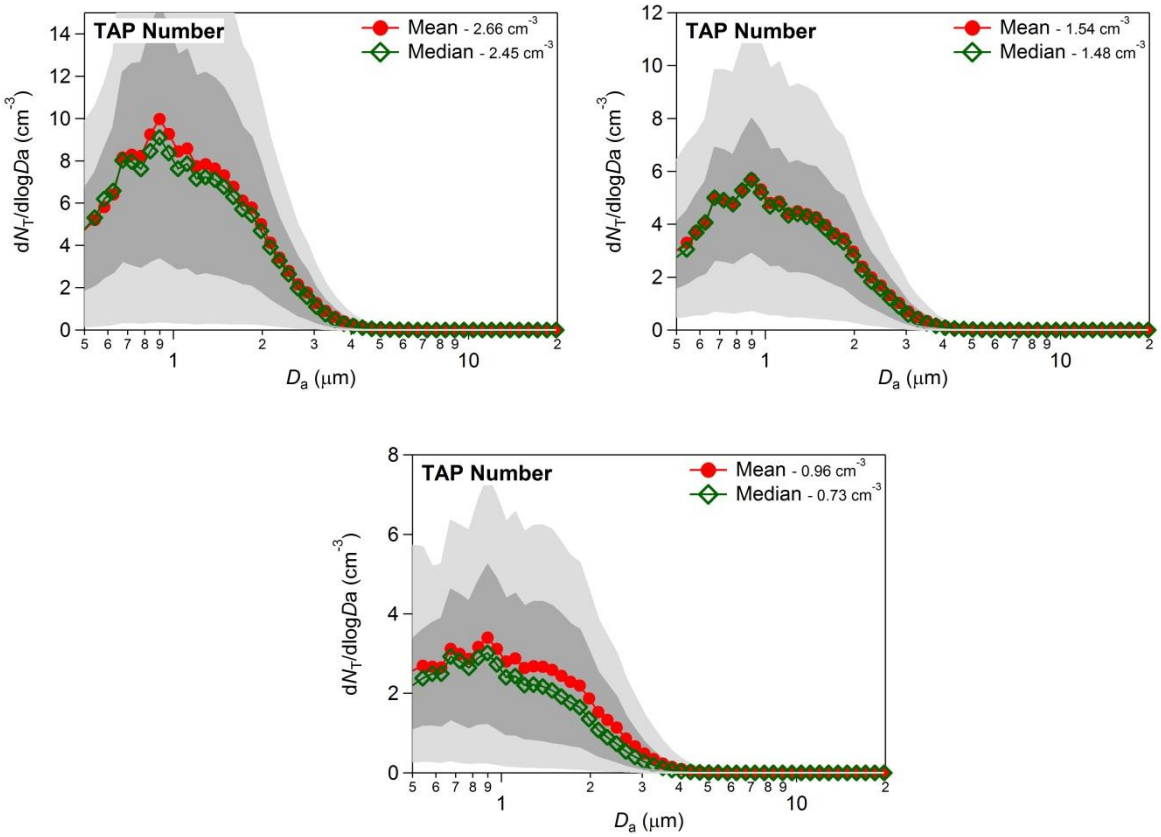

Fig S9: Unit-normalized TAP number size distribution averaged over the individual months (a) June, (b) July, and (c) August during the campaign.

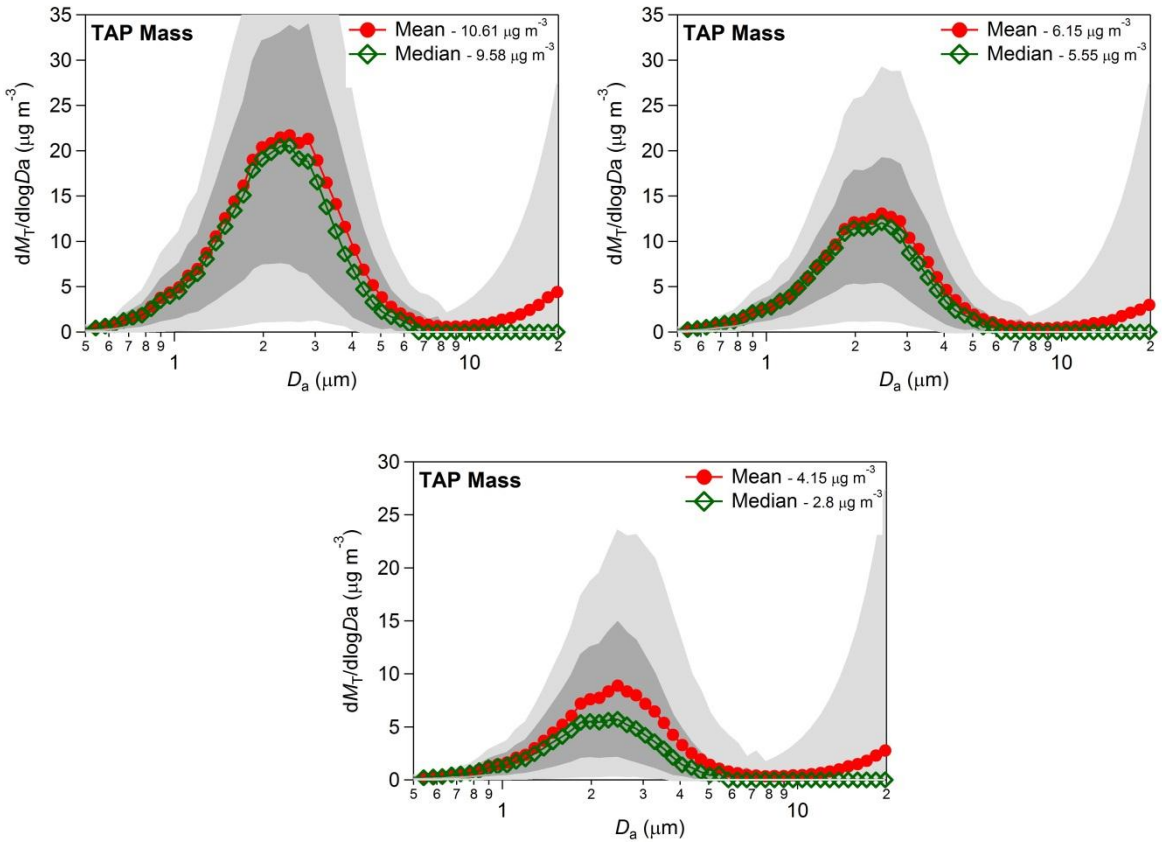

Fig S10: Unit-normalized TAP number size distribution averaged over the individual months (a) June, (b) July, and (c) August during the campaign.

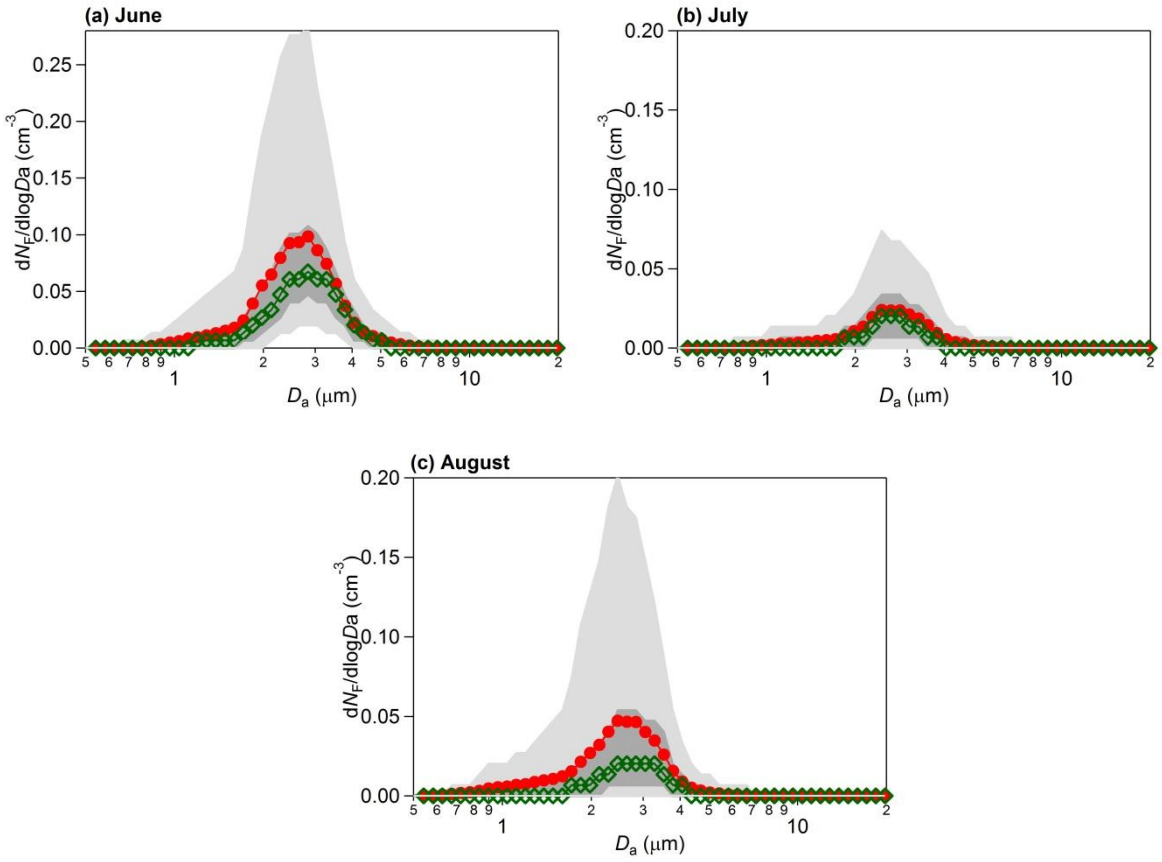

Fig S11: Same as Fig. 7b but representing only FBAP number ($dN_F/d\log D_a$) averaged over individual months (a) Jun, (b) Jul, and (d) Aug.

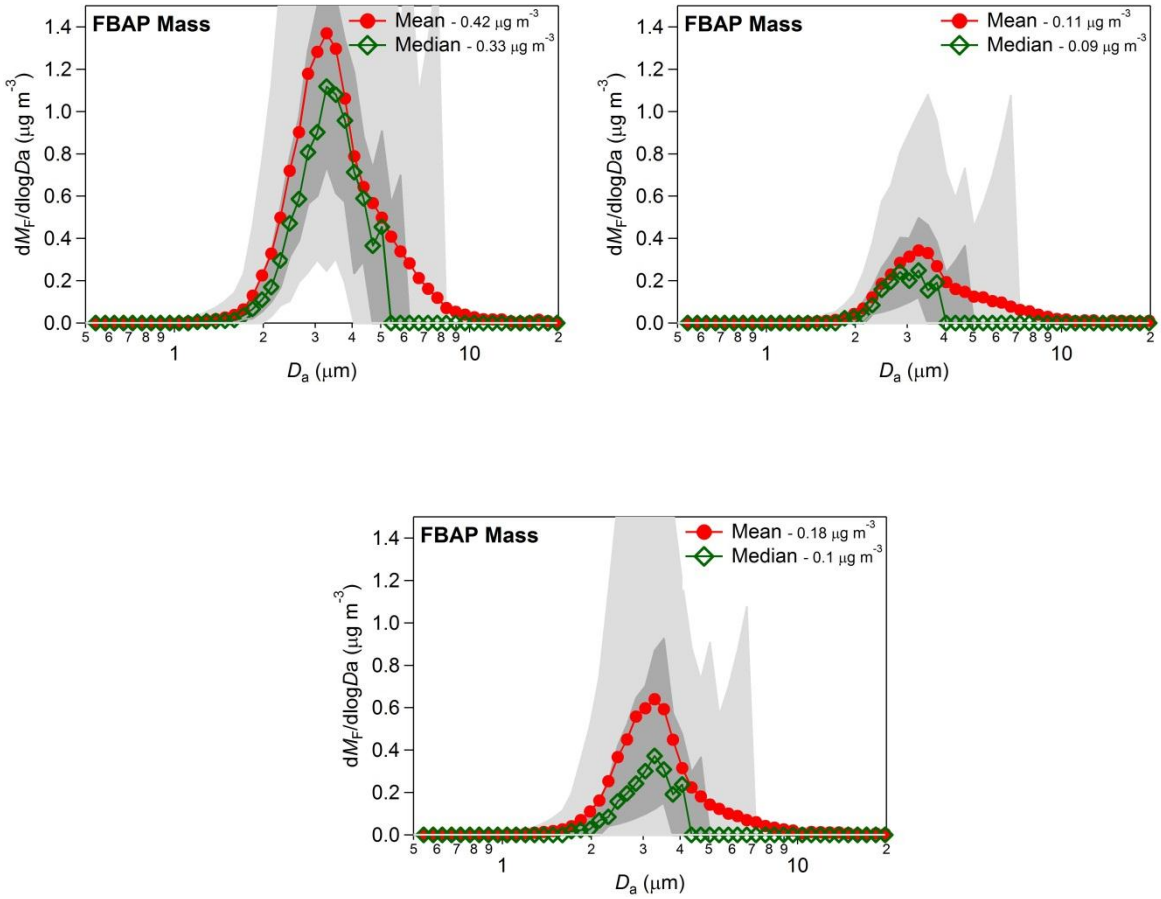

Fig. S12: Same as Fig. S11 but representing FBAP mass (dM_F/dlog D_a).

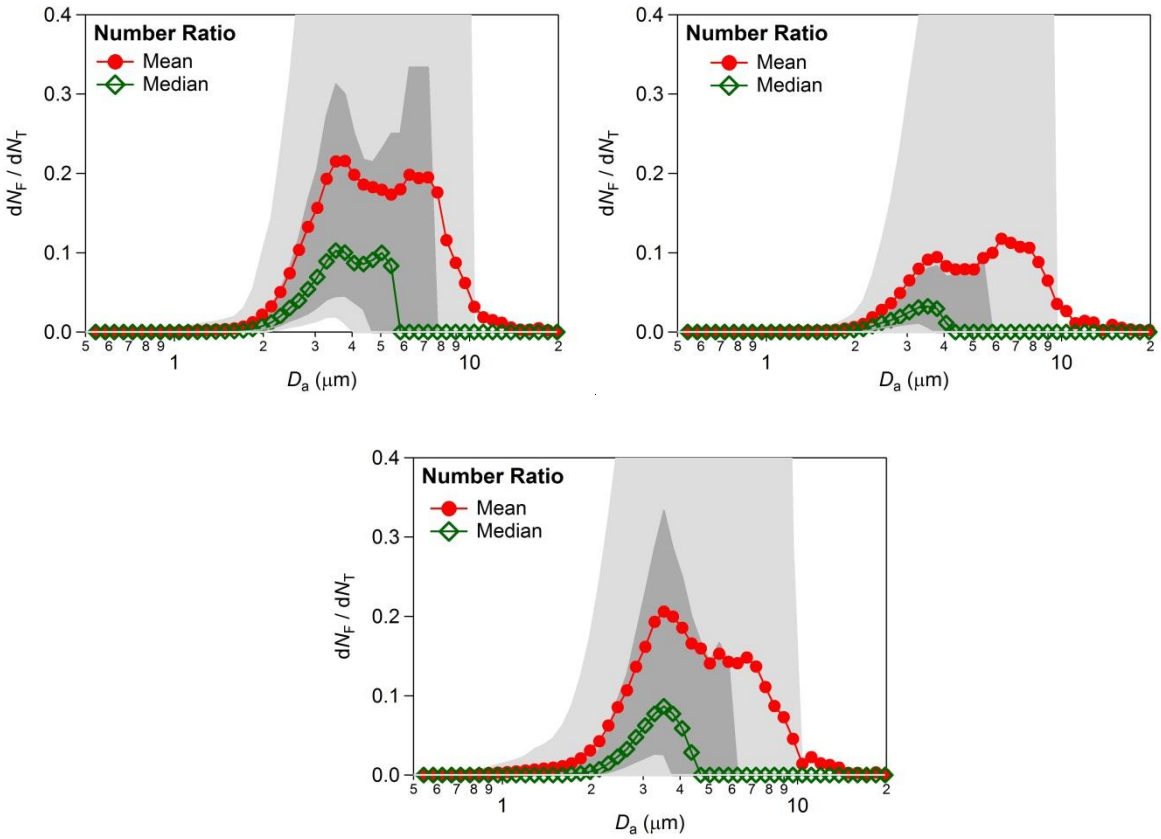

Fig S13: Size distribution of FBAP to TAP ratio averaged over each individual months (Jun-Aug) during the measurements carried out at Munnar ($dN_F/d\log D_a = dM_F/d\log D_a$).

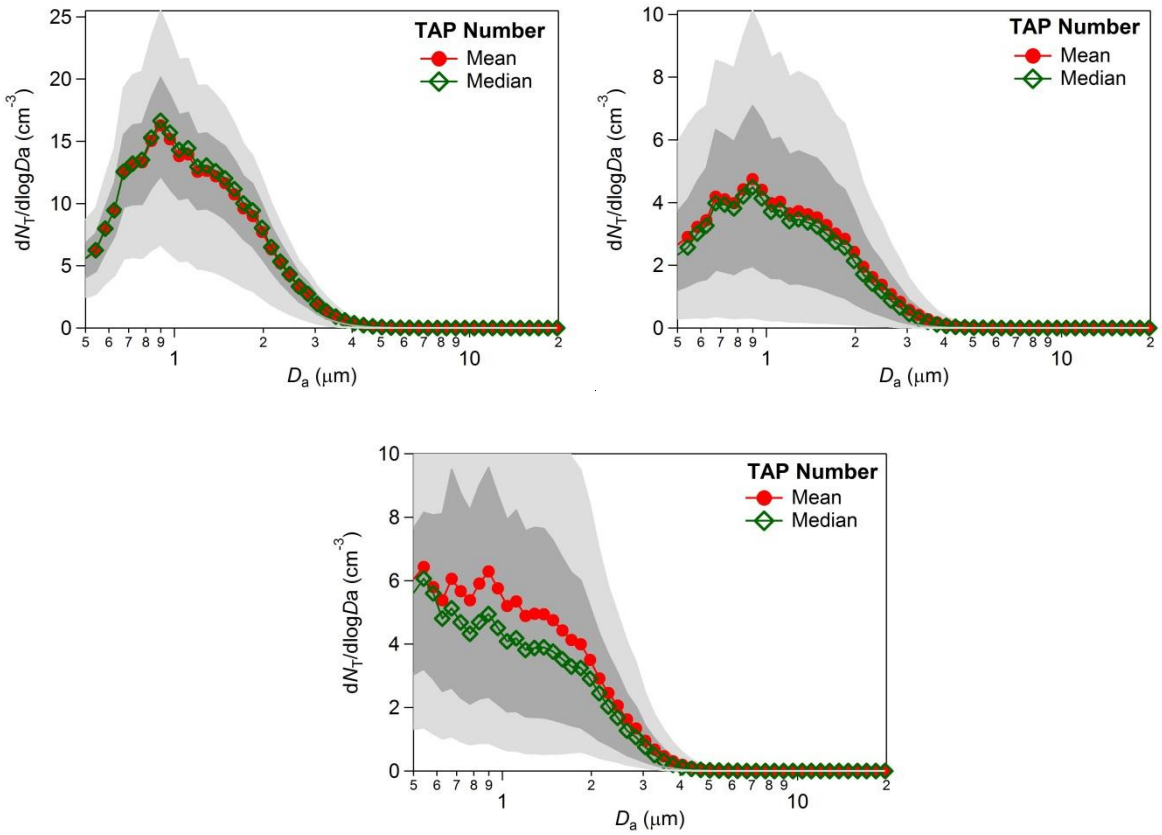

Fig S14: Unit-normalized TAP number size distribution averaged over the each distinct focus periods during the measurements carried out at Munnar.

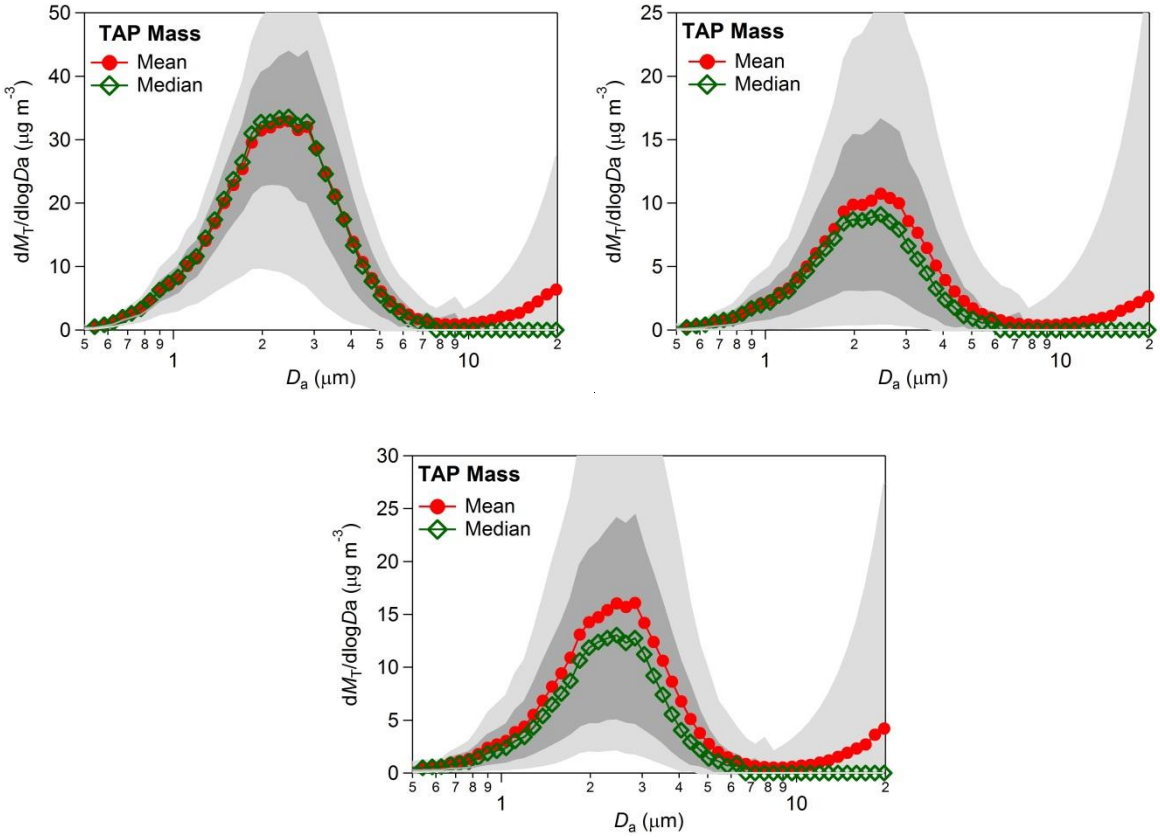

Fig S15: TAP mass size distribution averaged over the each distinct focus periods during the measurements carried out at Munnar.

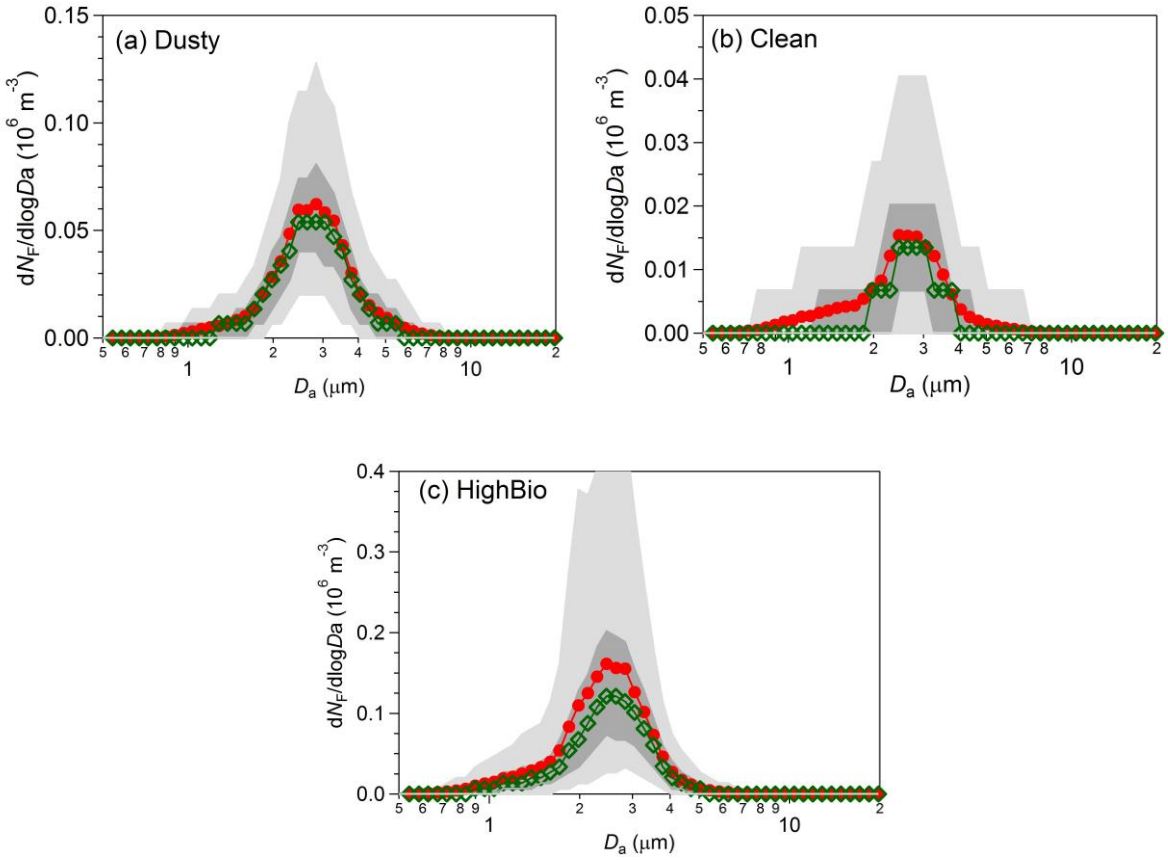

Figure S16: FBAP number size distributions (dN_F/dlog D_a) averaged over each distinct focus periods during the measurement campaign carried out at Munnar. Lower and upper parts of dark and light shaded area represent the 5th, 25th, 75th, and 95th percentile respectively. (a) dusty period , (b) clean period, and (c) high bio period.

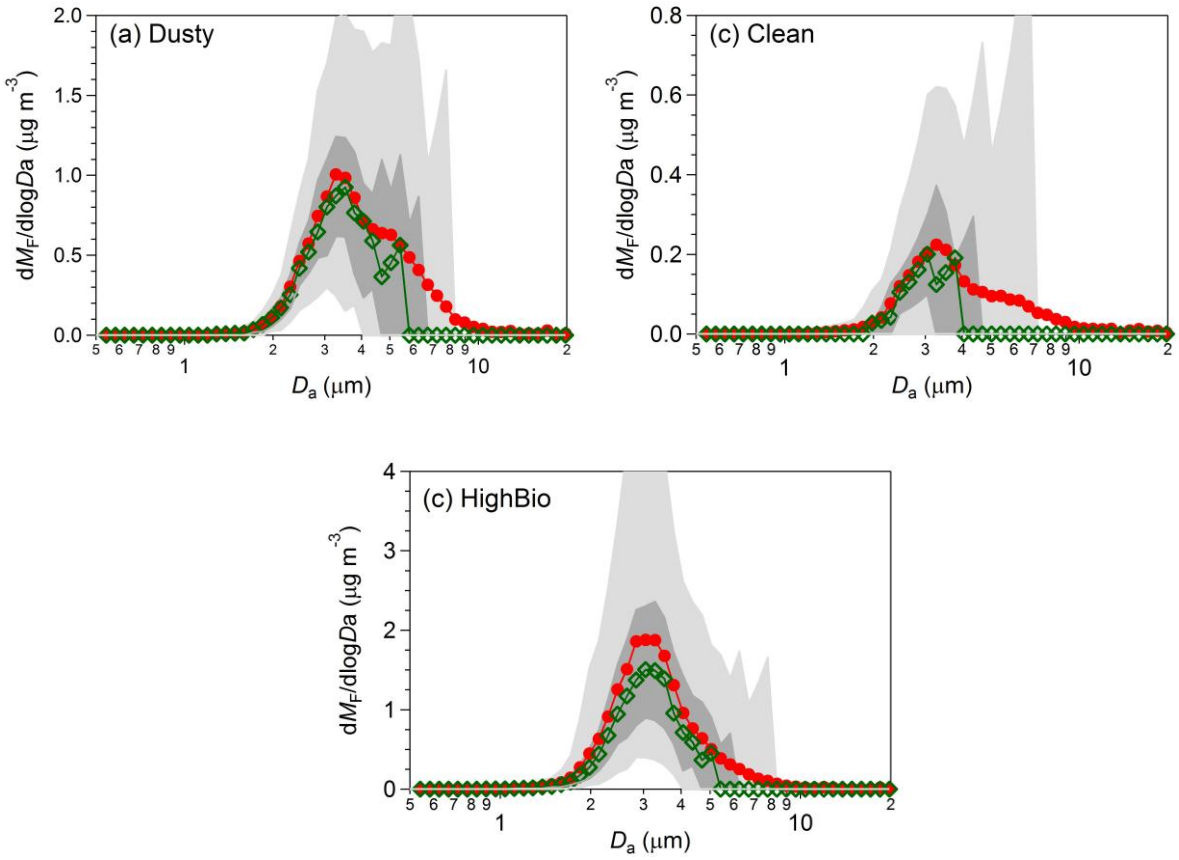

Figure S17: Same as Fig. S16 but representing FBAP mass size distribution (dM_F/dlog D_a).

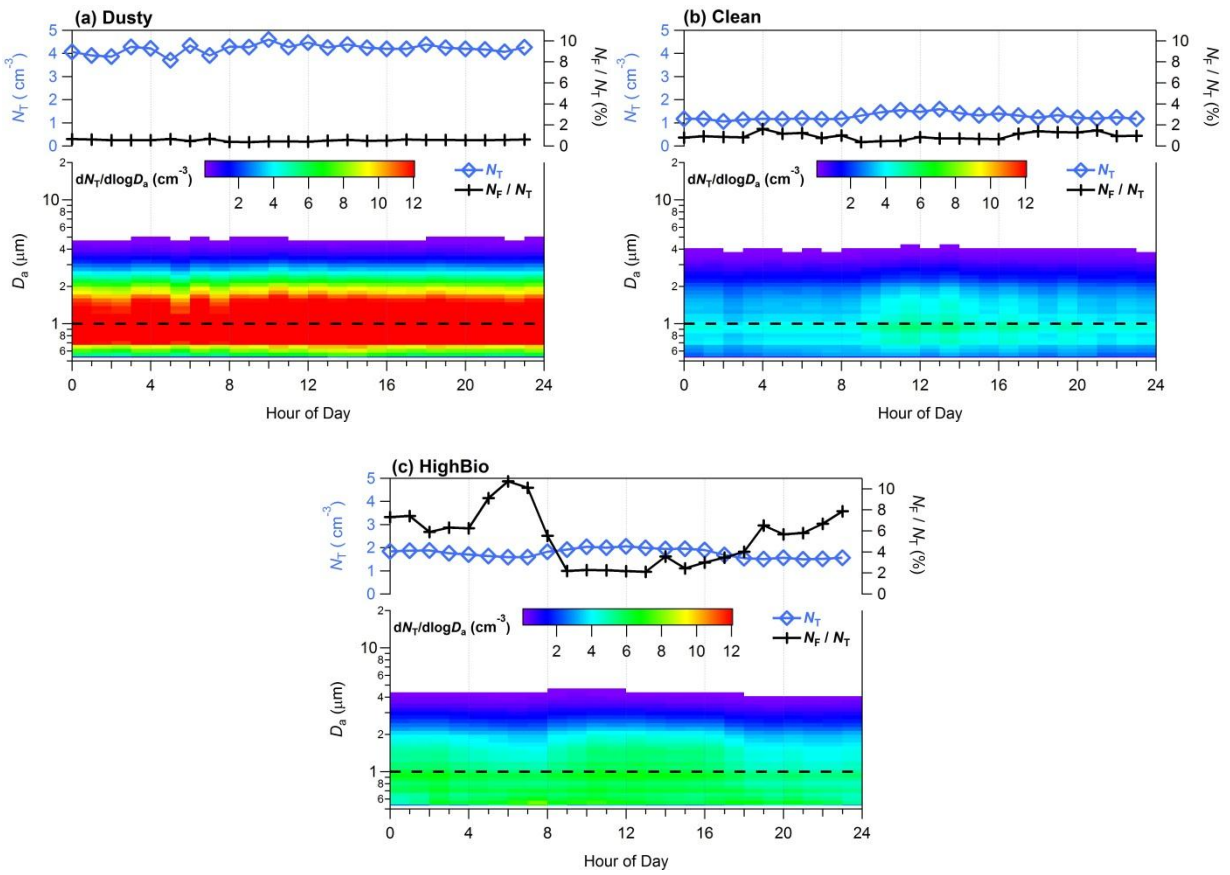

Fig S18: Diurnal cycles of TAP number concentrations (N_T) and size distributions averaged over each distinct focus periods (hourly median values plotted against the local time of the day).

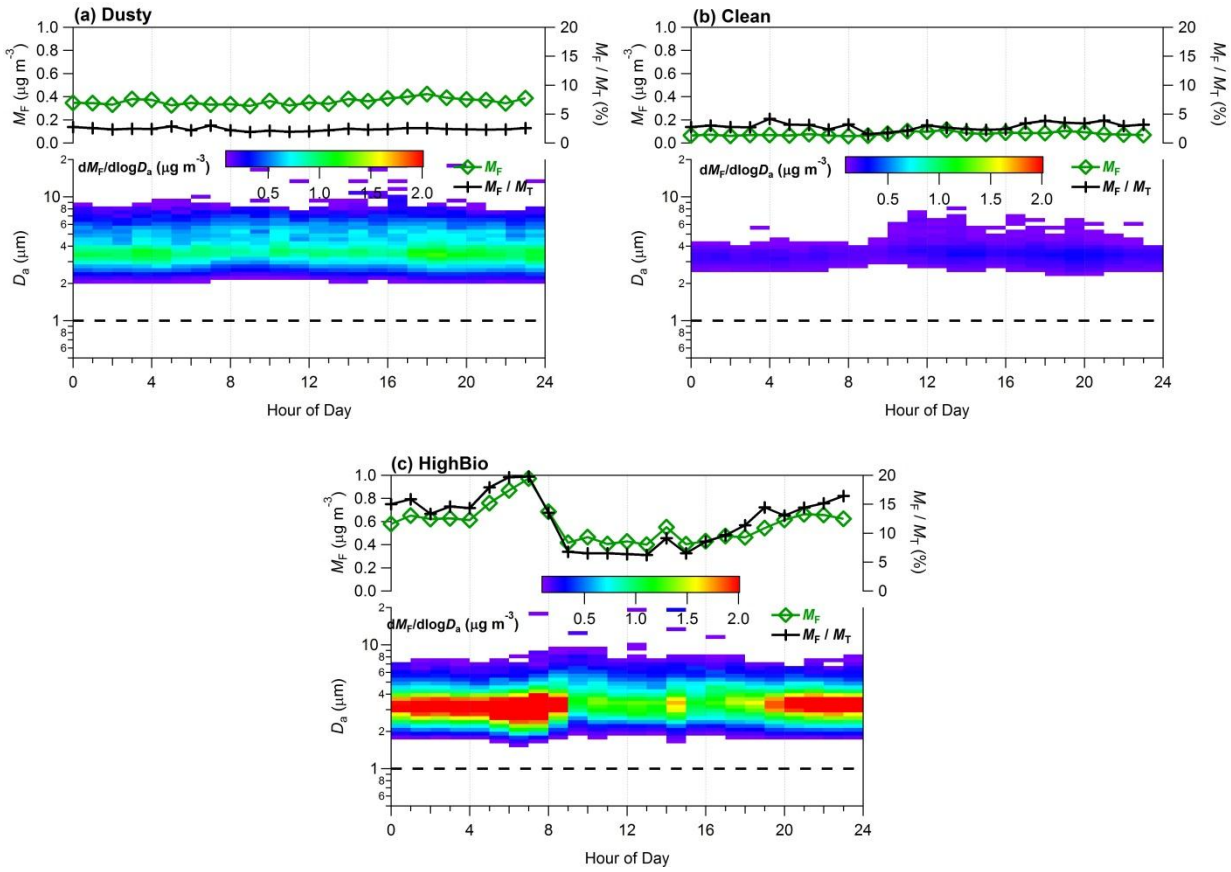

Fig S19: Same and Fig. 11 but representing the FBAP mass (M_F) concentration.

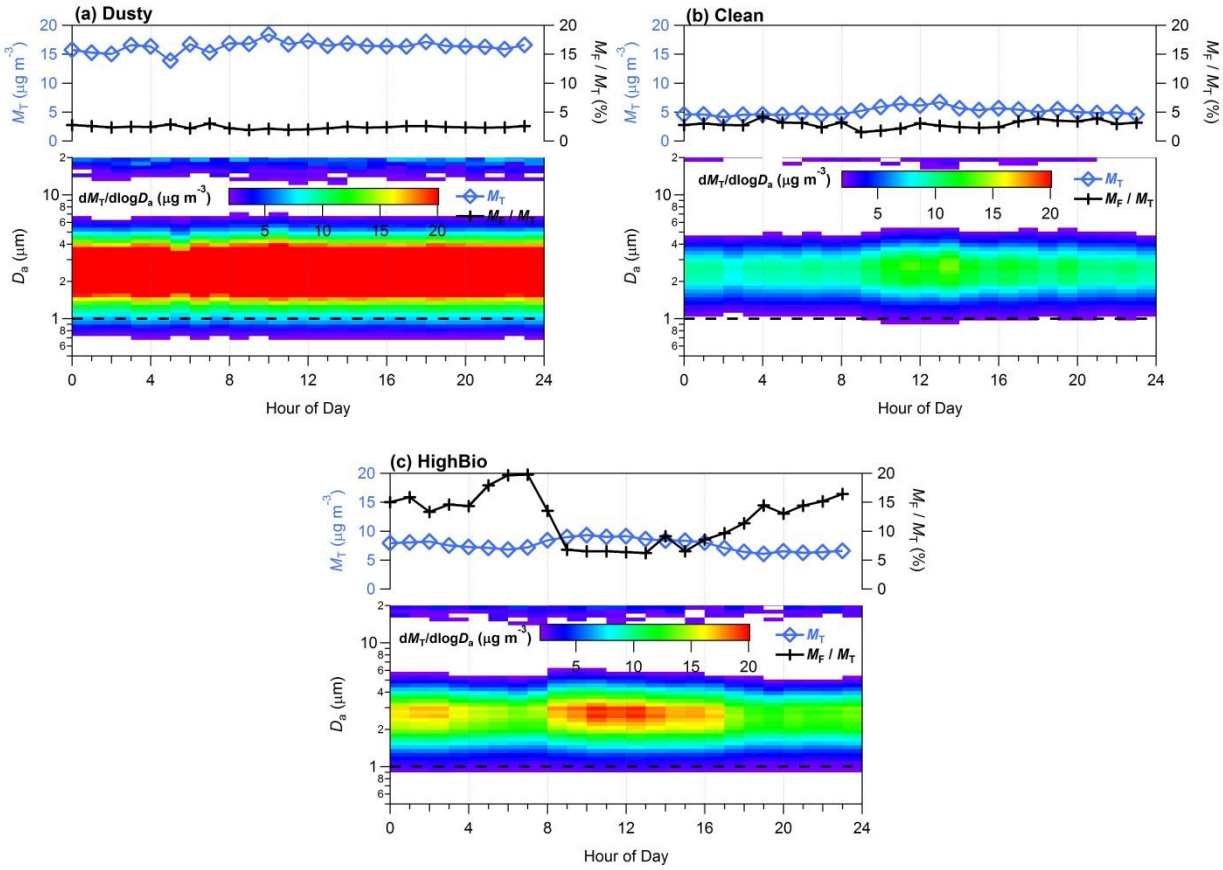

Fig S20: Diurnal cycles of TAP mass concentrations (M_T) and size distributions averaged over each distinct focus periods (hourly median values plotted against the local time of the day).

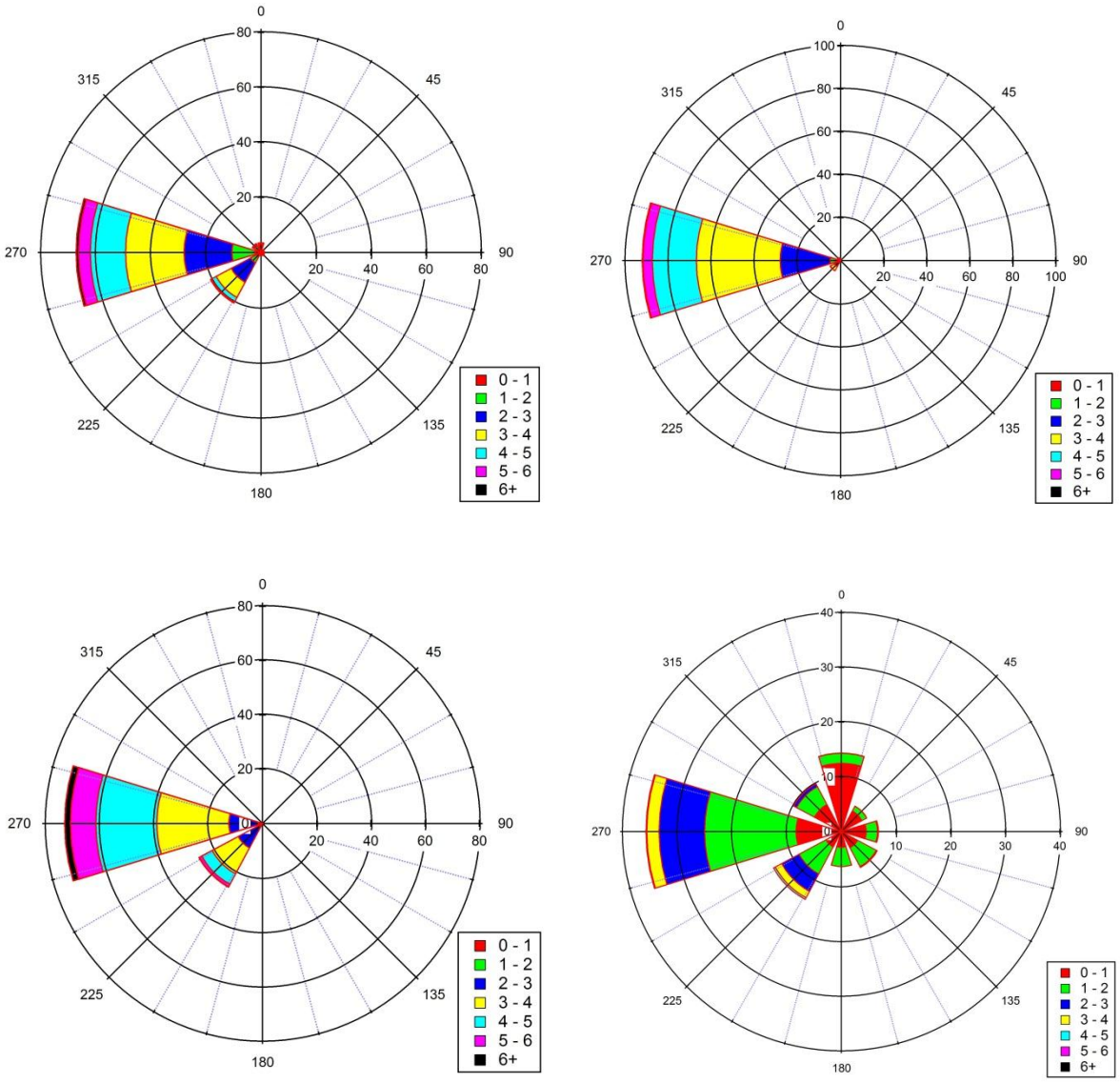

Fig S21: Wind rose diagram scaled over wind speed. (a) entire campaign, (b) dusty, (c) clean, and (d) high bio.

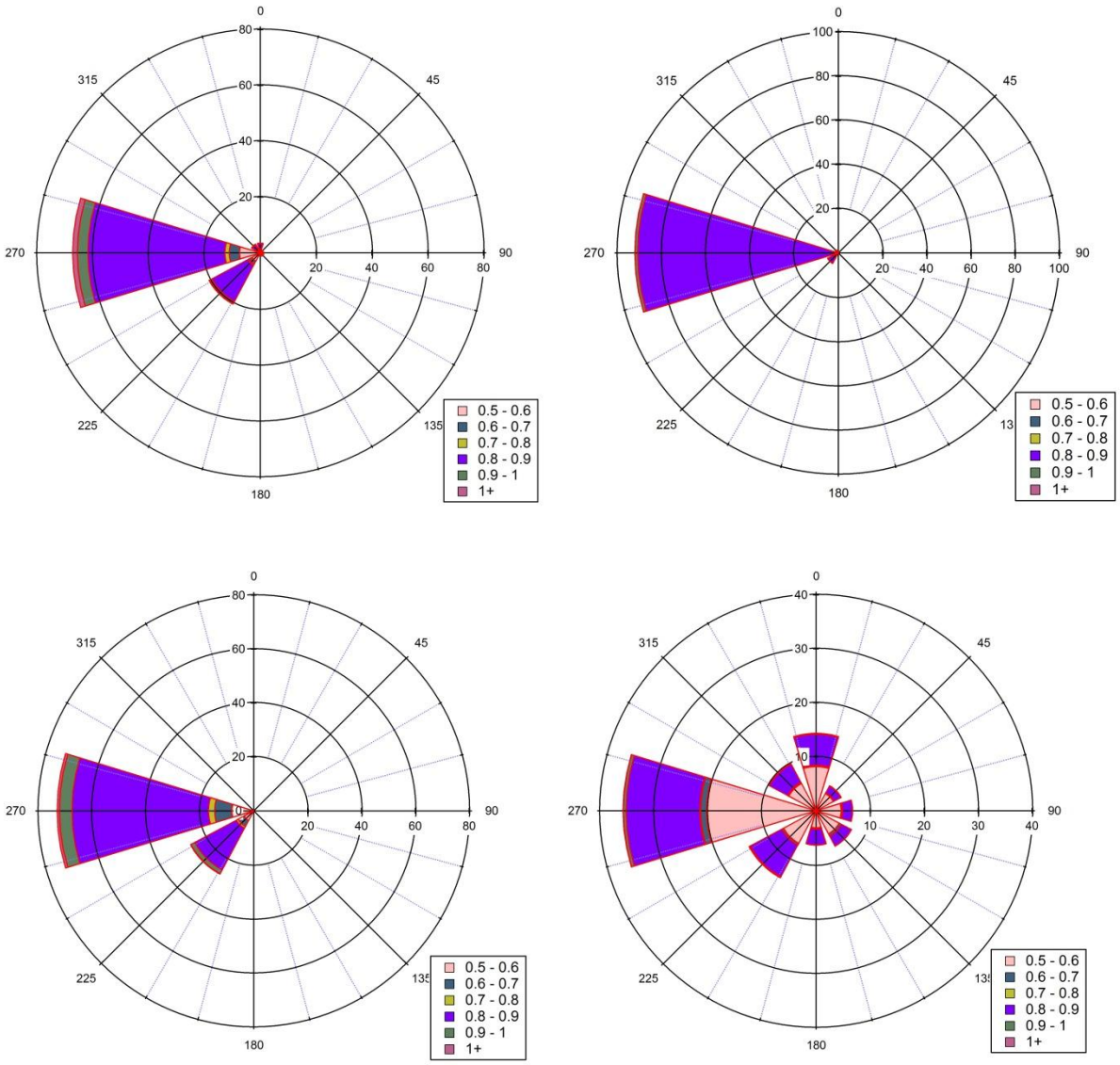

Fig S22: Wind rose diagram scaled by geometric mean diameter ($D_{g,T}$) of dN_T/dlog D_a. (a) entire campaign, (b) dusty period, (c) clean period, and (d) high bio period.

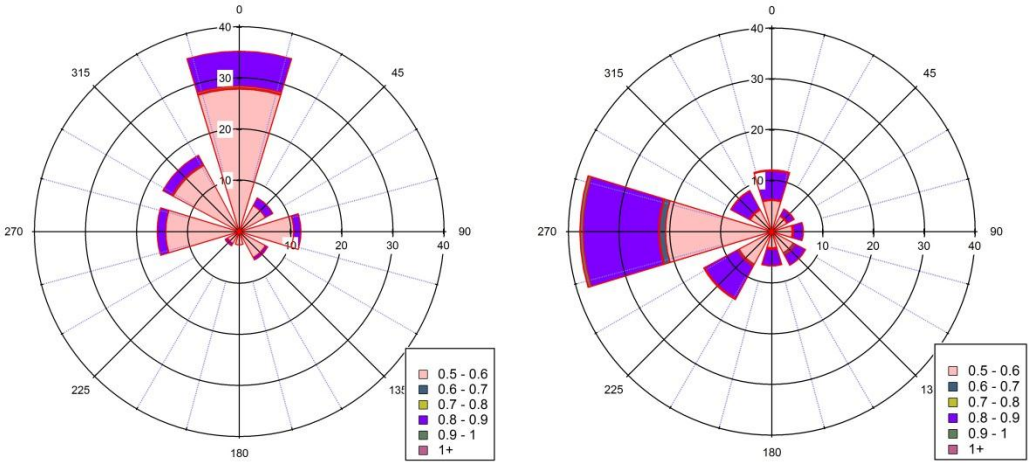

Fig S23: Wind rose diagram scaled by geometric mean diameter ($D_{g,T}$) of dN_T/dlog D_a, separated for FBAP number concentration (N_F) range, N_F>0.1 cm^{-3} (a) and N_F<0.1 cm^{-3} (b) observed during high bio period.